Am J Transl Res 2022;14(11):7744-7757
www.ajtr.org /ISSN:1943-8141/AJTR0144819

Original Article

The predictive value of pyroptosis for the prognosis and immune escape of bladder cancer

Yang Liu[1*], Zhong-Qi Pang[1*], Yan-Song Han[1], Lin-Kun Shen[1], Wen-Hao Yao[1], Lu Zhang[1], Jia-Xin He[1], Yu-Juan Shan[2], Ming-Hua Ren[1]

[1]Department of Urinary Surgery, First Affiliated Hospital of Harbin Medical University, Harbin 150007, Heilongjiang, China; [2]School of Public Health and Management, Wenzhou Medical University, Wenzhou 325000, Zhejiang, China. [*]Co-first authors.

Received June 17, 2022; Accepted September 28, 2022; Epub November 15, 2022; Published November 30, 2022

Abstract: Objective: To evaluate the predictive value of pyroptosis-related genes for the prognosis and immune escape of bladder cancer (BC). Methods: Transcriptomic and single nucleotide polymorphisms (SNPs) data were downloaded from The Cancer Genome Atlas (TCGA) and Gene Expression Omnibus (GEO) portal. Least absolute shrinkage and selection operator (LASSO) analysis was carried out to construct a prognostic risk model for BC patients. Results: Based on the expression of 50 pyroptosis-related genes, BC patients from TCGA database were divided into two clusters, which showed significant differences in overall survival and disease specific survival. Furthermore, we intersected the differentially expressed genes between these two clusters with those identified from the GSE13507 dataset and finally identified eight survival related genes, which was used to construct a prognostic risk model by LASSO Cox regression. According to the model, the high-risk (HR) group was closely associated with poor survival or the advanced pathological stage of BC. In addition, the HR group was mainly enriched in cell cycle and immune-related pathways and had a higher TP53 mutation rate than the low-risk (LR) group. Furthermore, these two risk groups were significantly related to immune cell composition, immune cell infiltration, and immune response. Importantly, a higher expression of PD-1, PD-L1, and CTLA4 as well as higher immune exclusion scores were found in the HR group, suggesting a higher possibility of immune escape. Conclusion: Our studies revealed the key role of pyroptosis in predicting the prognosis, TP53 mutation, and immune escape of patients with BC.

Keywords: Pyroptosis, bladder cancer, prognosis, immunotherapeutic, risk model

Introduction

Bladder cancer (BC) is the most commonly diagnosed malignancy of urinary system worldwide [1, 2]. The known risk factors for BC include sex, age, race, chemicals, radiation, drugs, chronic infection, genetics, and smoking [3]. Despite the advancement on current treatment options such as surgery, chemotherapy, and molecular targeted therapy, many patients still experience unsatisfactory therapeutic outcomes, and the incidence and mortality of BC are increasing in recent years [4]. Therefore, it is imperative to explore novel effective therapeutic methods and molecular targets to improve the prognosis of BC.

Pyroptosis is a type of programmed cell death associated with inflammation, as some inflammasomes can activate caspase-1, 4, 5, 11 to initiate the process of pyroptosis [5]. The phenotypic changes in cells undergoing pyroptosis include cytoplasmic swelling, chromatin fragmentation, cell membrane perforation, the generation of intracellular proinflammatory cytokines, and, finally, the leakage of cytosolic contents [6]. During tumor development, pyroptosis has been found to play dual roles as either inhibiting or promoting tumorigenesis via different mechanisms [7]. Furthermore, pyroptosis has been associated with prognosis of BC, and pyroptosis-related genes affect the formation of the tumor immune microenvironment in BC [8]. However, the role of pyroptosis in the prognosis and the immunity of BC remain to be elucidated, and the systematic and comprehensive understanding of the predictive value of pyroptosis is still limited [9].

Immune escape leads to different outcomes in bladder cancer and has been closely associated with immune checkpoints [10]. Accumulating evidence has indicated that the expression of PD-1, PD-L1 and CTLA4 dictates the efficacy of immunotherapy in BC [11]. At present, several immune checkpoint inhibitors such as MPDL3280A (an anti-PD-L1 drug) have been approved for the treatment of BC by The Food and Drug Administration (FDA) and have shown significant antitumor activity in metastatic BC [12]. Therefore, stratifying patients with high expression of immune checkpoints can improve the efficacy of immunotherapy in BC. On the other hand, gene mutations can also be used to predict cancer prognosis. For example, TP53 is one of the most commonly mutated genes in cancer, and TP53 mutation promotes tumor development and results in poor overall survival [13, 14]. In addition, KMT2D mutations are also associated with the poor prognosis of patients with cancer [15]. These data indicate the importance of accurately identifying patients with gene mutation in the precision treatment of BC.

Therefore, this study aimed to establish a molecular model that could reliably predict the prognosis, gene mutations, and immune escape based on the pyroptosis-related genes in BC, and provide novel potential molecular targets for the treatment of patients with BC.

Materials and methods

Data collection

The transcriptome data, SNPs data, and the related clinical information of 430 samples (411 BC patients and 19 normal samples) were downloaded from the TCGA database (https://tcga-data.nci.nih.gov/tcga/). In addition, the transcriptome data and the clinical information of 187 BC patients were acquired from the GEO database (http://www.ncbi.nlm.nih.gov/geo/).

Identification of differentially expressed genes

We first normalized all transcriptomics data by log2(x+1). Then, we utilized the R package with FDR<0.05 and |log2FC| ≥1 to identify differentially expressed genes (DEGs) in both TCGA and GEO cohorts.

Protein-protein interaction network

We explored the protein-protein interaction network (PPI) for pyroptosis-related genes by using STRING (https://string-db.org/) and Cytoscape software.

Functional enrichment analysis

We utilized gene set enrichment analysis (GSEA) (http://www.gsea-msigdb.org/gsea/index.jsp) and the Database for Annotation, Visualization and Integrated Discovery (DAVID) (https://david.ncifcrf.gov/) to perform gene ontology (GO) and Kyoto Encyclopedia of Genes and Genomes (KEGG) enrichment analyses for different risk groups.

Establishment of the prognostic risk model

We first performed univariate Cox analysis to determine the survival related DEGs in both TCGA and GEO cohorts. After cross-validation of the two datasets, eight genes associated with survival were identified. Next, we established a prognostic risk model by performing the LASSO Cox regression. The risk score was calculated by the formula: $\sum_i^8$ Ai × Bi (A: coefficients, B: gene expression level). Finally, all samples from both TCGA and GEO cohorts were divided into low-risk (LR) and high-risk (HR) groups according to the risk score for further analysis.

Statistical analysis

We employed one-way ANOVA and t test for comparison between LR and HR groups, and the comparison of two or more constituent ratios was tested by chi-square test. Kaplan-Meier analysis was used to estimate the survival of patients in different risk groups. Spearman test was used for correlation analysis. The receiver operating characteristic curve (ROC) was used to evaluate the prediction efficiency of our model. Heat map, waterfall curve, and box plots were visualized by R software (version 3.5.1). We processed all statistical analyses by SPSS 19.0 software (SPSS. Inc., Chicago, IL, USA) or R software. P<0.05 was considered statistically significant.

Results

Pyroptosis-related genes could predict the prognosis in BC

Based on our literature review, we first selected 50 pyroptosis-related genes and analyzed their expression levels in 430 samples, including 411 BC and 19 normal samples, from the TCGA database. We found that 72% (36/50) pyroptosis-related genes, especially AIM2 and HMGB1,

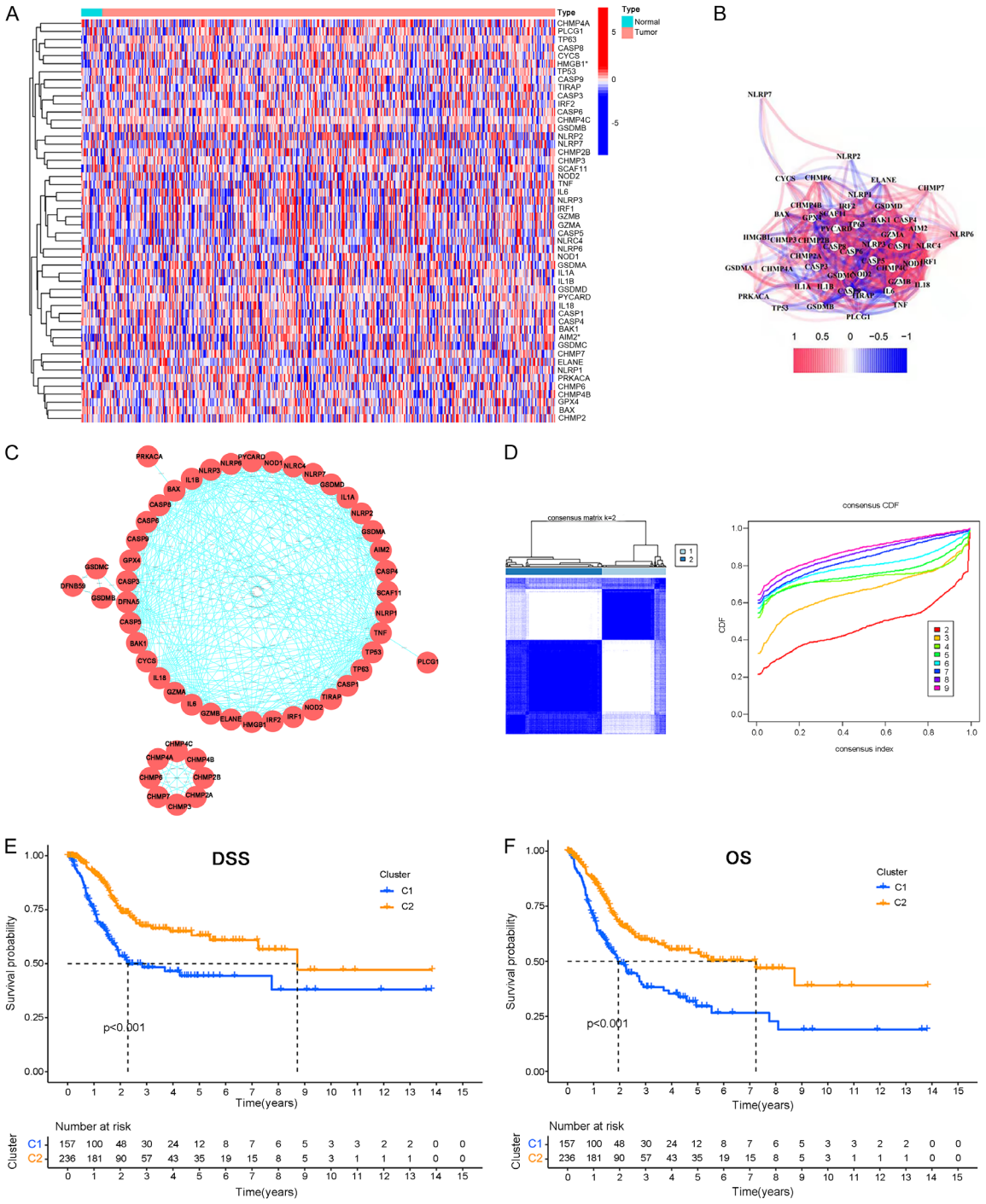

Figure 1. The expression of pyroptosis-related genes could distinguish the prognosis in bladder cancer. (A) Heatmap of pyroptosis-related genes expression between normal and BC samples in TCGA cohort. (B) The correlation network of Pyroptosis-related genes. (C) The protein-protein interaction network of pyroptosis-related genes. (D) BC samples (n=411) were divided into two clusters based on the consensus clustering matrix (k=2) in TCGA cohort. (E, F) Kaplan-Meier analysis of DSS (E) and OS (F).

were upregulated in BC when compared with normal samples (**Figure 1A**). In addition, these pyroptosis-related genes exhibited a strong protein-protein interaction and correlations among them (**Figure 1B**, **1C**). These findings suggested that pyroptosis-related genes were coordinated with each other and involved in BC.

To further explore the influence of pyroptosis on the prognosis of BC, we performed a consen-

sus clustering analysis on these 50 pyroptosis-related genes. We found that when the clustering variable (k) was 2 (cluster C1 and C2), the BC samples could be well separated (**Figure 1D**). Samples in C2 had higher survival probability in both disease-specific survival (DSS) and overall survival (OS) than samples in C1 (P<0.001) (**Figure 1E**, **1F**), suggesting that these pyroptosis-related genes were related to the prognosis of patients with BC.

A risk model for the prognosis of BC patients

Based on the results from gene cluster analysis, 230 DEGs were identified between the LR and HR groups of TCGA samples, of which 72 were considered as survival-related genes since their expression was clearly associated with DSS (**Figure 2A**; Supplementary Table 1). Next, we intersected these survival-related genes with those obtained from the 187 BC samples in GSE13507 dataset and identified eight survival-related genes (KRT1, DSG3, PCOLCE2, ALDH1L2, CTSE, SULT1E1, GSDMB, BCL2L14). We further performed LASSO cox regression analysis to establish an 8-gene risk model based on the optimum λ value (**Figure 2B**, **2C**). Moreover, we calculated the risk score of each sample using the formula: Risk score = (0.06 * expression of KRT1) + (0.05 * expression of DSG3) + (-0.68 * expression of BCL2L14) + (0.12 * expression of ALDH1L2) + (-0.05 * expression of CTSE) + (-0.01 * expression of SULT1E1) + (-0.23 * expression of GSDMB) + (0.06 * expression of PCOLCE2).

According to the median risk score, the 393 BC patients in TCGA cohort with complete survival information were separated into high-risk (HR) and low-risk (LR) groups (Supplementary Figure 1A). Compared with LR group, the patients in HR group had high mortality rate and shorter overall survival (Supplementary Figure 1B). Furthermore, principal component analysis (PCA) and t-distributed stochastic neighbor embedding (t-SNE) analyses indicated that patients in these two risk groups could be well separated (Supplementary Figure 1C, 1D). Kaplan-Meier analysis for DSS indicated that patients in the HR group had higher mortality rate than patients in the LR group (P<0.001, **Figure 2D**). The predictive power of our risk model on DSS was validated by receiver operating characteristic (ROC) analysis, as the area under the ROC curve (AUC) was 0.737, 0.708 and 0.697 for 1-, 3-, 5-year survival, respectively (**Figure 2H**).

Moreover, patients in the HR group had worse OS and progression-free survival (PFS) than patients in the LR group (P<0.001, **Figure 2E**, **2G**); however, there was no obvious difference in disease free survival (DFS) between these two groups (P=0.704, **Figure 2F**). To further validate the predictive power of our model, ROC analysis for OS and PFS was conducted. Consistently, AUC value was 0.691, 0.701 and 0.682 for 1-, 3-, 5-year OS, respectively (**Figure 2I**), while AUC value was 0.724, 0.624 and 0.623 for 1-, 3-, 5-year PFS, respectively (**Figure 2J**). Together, these data demonstrated the superior predictive power of our risk model for the survival of BC patients.

The HR group predicted poor clinical features of BC patients

We first created the heatmap of samples from TCGA cohort to demonstrate the expression of the eight survival-related genes in the two risk groups. The data showed that the expression of KRT1, DSG3, PCOLCE2 and ALDH1L2 genes was higher in the HR group than in the LR group, while the expression of CTSE, SULT1E1, GSDMB and BCL2L14 genes was lower in the HR group than in the LR group (**Figure 3A**). Next, we investigated the correlation between the clinical characteristics and the risk groups in TCGA cohort. We found that the clinical features such as race, diagnosis subtype, neoplasm histologic grade and tumor stage were strongly associated with the risk scores (P<0.05) (**Figure 3B**). Although most BC patients with stage 2 or 3 tumors were evenly distributed in both risk groups (73% in LR group and 61% in HR group), more patients with tumor stage 4 were in HR group than in LR group (39% vs 26%) (P=0.001) (**Figure 3C**). Similar results were obtained in GEO cohort (**Figure 4A**). And clinical features such as invasiveness status, tumor grade, and tumor progression status were also strongly associated with risk scores (**Figure 4B**). Likewise, the number of patients with high tumor grade was much higher in the HR group than in the LR group (56% vs 19%) (P=0.001) (**Figure 4C**). Furthermore, we also investigated the T stage profiles of patients in these two risk groups using the GEO cohort and found that more patients with lower tumor stage (Ta and T1) were in the LR group than in the HR group (46% vs 79%) (**Figure 4D**). Collectively, these results demonstrated that HR group predicted poor clinical prognosis.

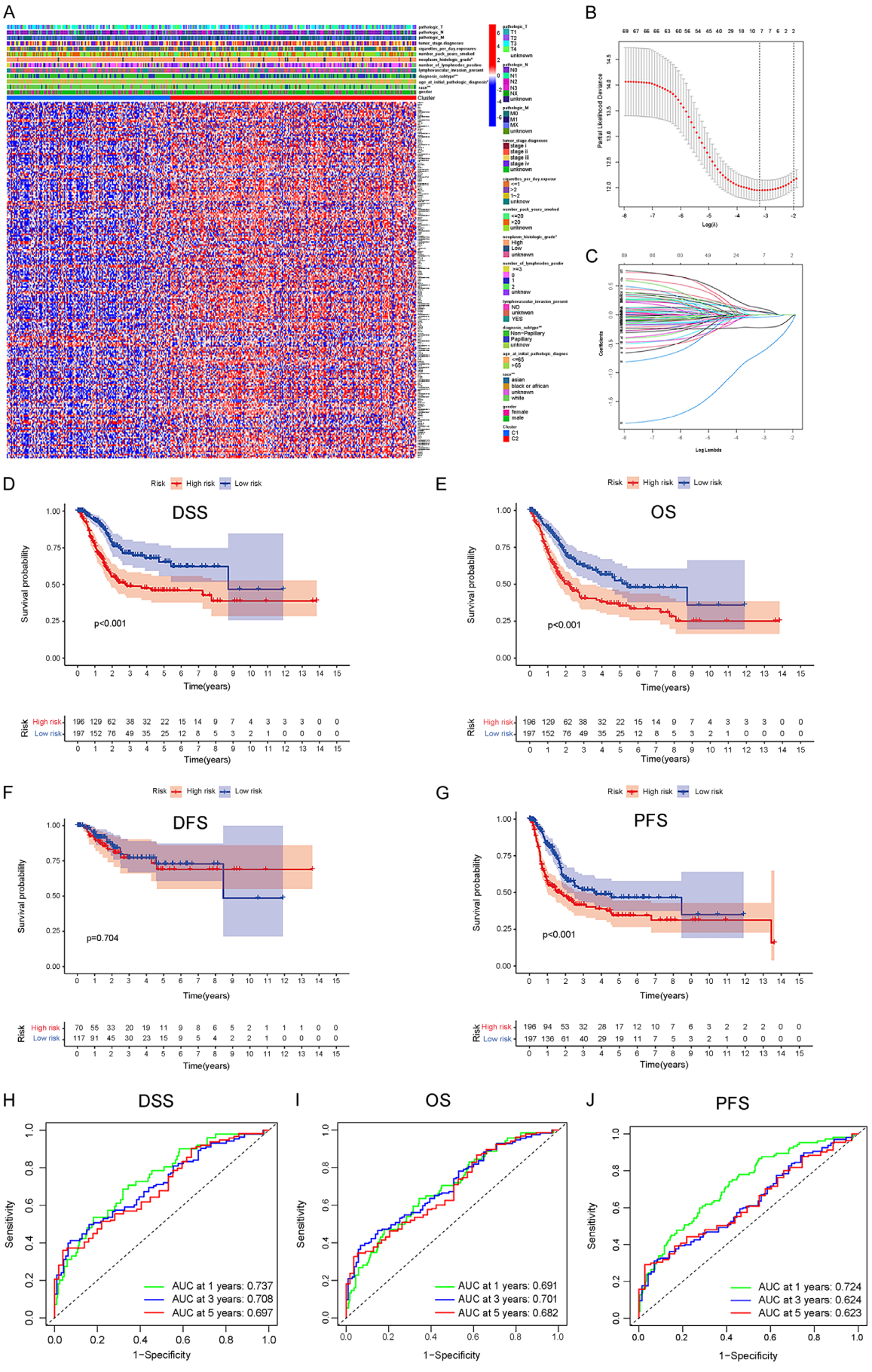
A
B
C
D
DSS
Risk High risk Low risk
Survival probability
p<0.001
Time(years)
High risk 196 129 62 38 32 22 15 14 9 7 4 3 3 3 0 0
Low risk 197 152 76 49 35 25 12 8 5 3 2 1 0 0 0 0
E
OS
p<0.001
High risk 196 129 62 38 32 22 15 14 9 7 4 3 3 3 0 0
Low risk 197 152 76 49 35 25 12 8 5 3 2 1 0 0 0 0
F
DFS
p=0.704
High risk 70 55 33 20 19 11 9 8 6 5 2 1 1 1 0 0
Low risk 117 91 45 30 23 15 9 5 4 2 2 1 0 0 0 0
G
PFS
p<0.001
High risk 196 94 53 32 28 17 12 10 7 6 3 2 2 2 0 0
Low risk 197 136 61 40 29 19 11 7 5 3 2 1 0 0 0 0
H
DSS
Sensitivity
1−Specificity
AUC at 1 years: 0.737
AUC at 3 years: 0.708
AUC at 5 years: 0.697
I
OS
AUC at 1 years: 0.691
AUC at 3 years: 0.701
AUC at 5 years: 0.682
J
PFS
AUC at 1 years: 0.724
AUC at 3 years: 0.624
AUC at 5 years: 0.623

Figure 2. Construction of a prognostic risk model based on the data from TCGA and GEO. A. Heatmap of gene expression of different classification in TCGA cohort. B. LASSO Cox regression analysis for the 8 survival-related genes in both TCGA and GEO cohorts. C. Cross-validation between TCGA and GEO cohorts in the LASSO regression. D-G. Kaplan-Meier analysis for DSS, OS, DFS, PFS in risk groups, respectively. H-J. ROC analysis was used to verify the predictive efficiency of the risk model for DSS, OS and PFS, respectively.

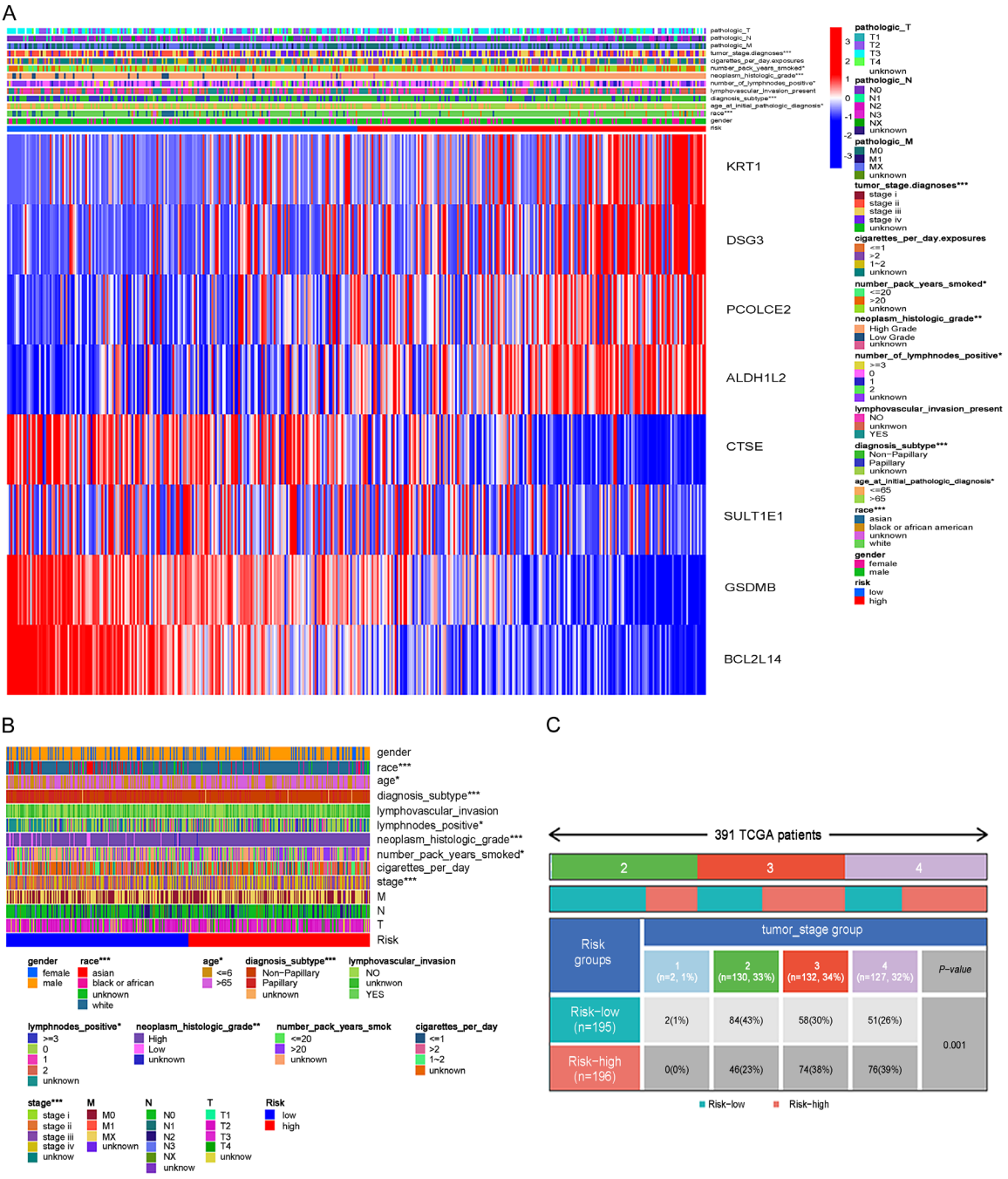

Figure 3. The HR group predicted the poor clinical features of BC patients. A. Heatmap of the 8 survival-related genes expression levels in the HR and LR groups in TCGA cohort. B. Heatmap of the correlation of clinical characteristics with risk groups in TCGA cohort. C. Chi-square test for tumor T stages and risk groups of BC patients in TCGA cohort.

A

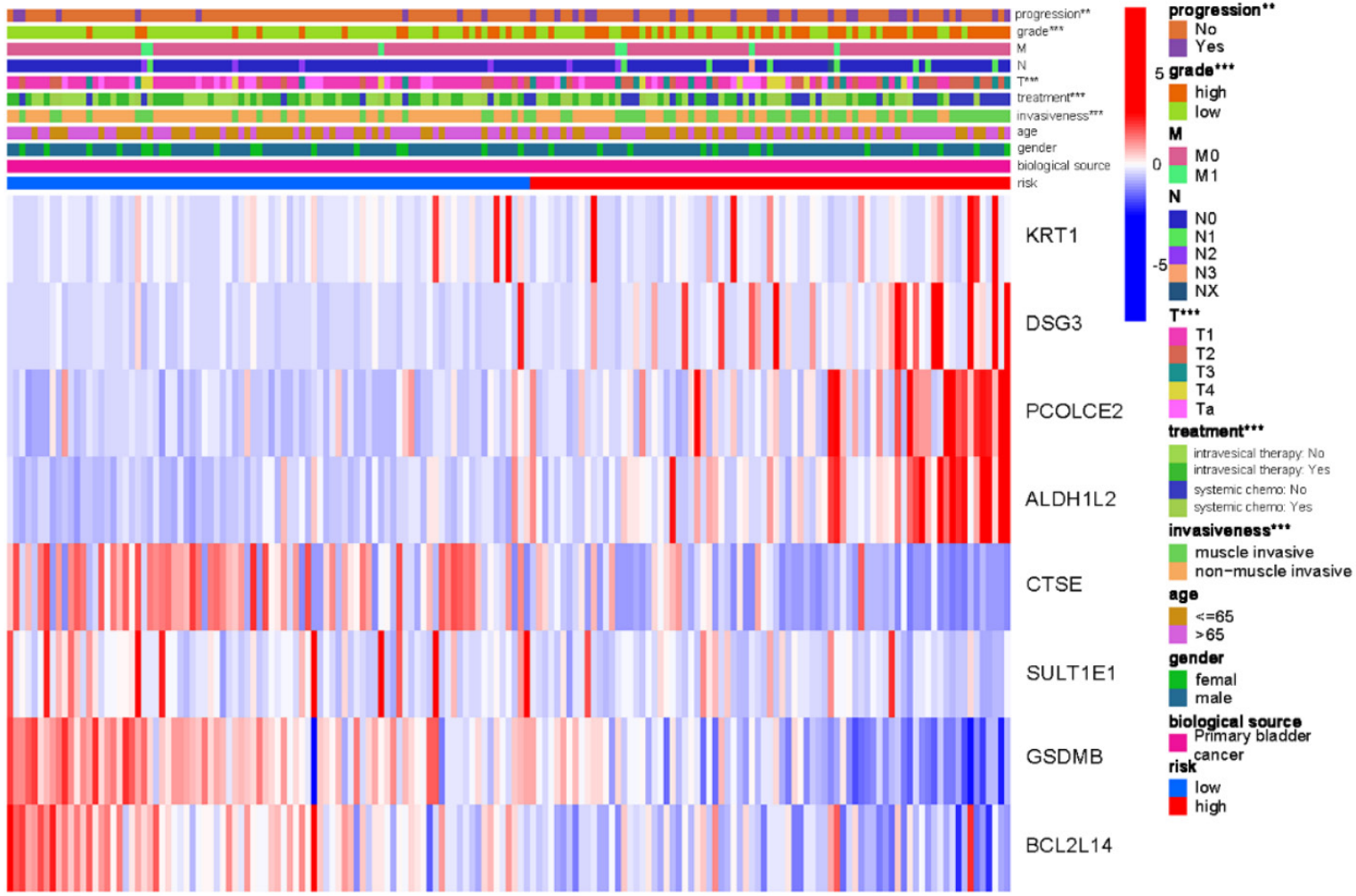
progression**
grade***
M
N
T**
treatment***
invasiveness***
age
gender
biological source
risk
KRT1
DSG3
PCOLCE2
ALDH1L2
CTSE
SULT1E1
GSDMB
BCL2L14
5
0
-5
progression**
No
Yes
grade***
high
low
M
M0
M1
N
N0
N1
N2
N3
NX
T***
T1
T2
T3
T4
Ta
treatment***
intravesical therapy: No
intravesical therapy: Yes
systemic chemo: No
systemic chemo: Yes
invasiveness***
muscle invasive
non−muscle invasive
age
<=65
>65
gender
femal
male
biological source
Primary bladder cancer
risk
low
high

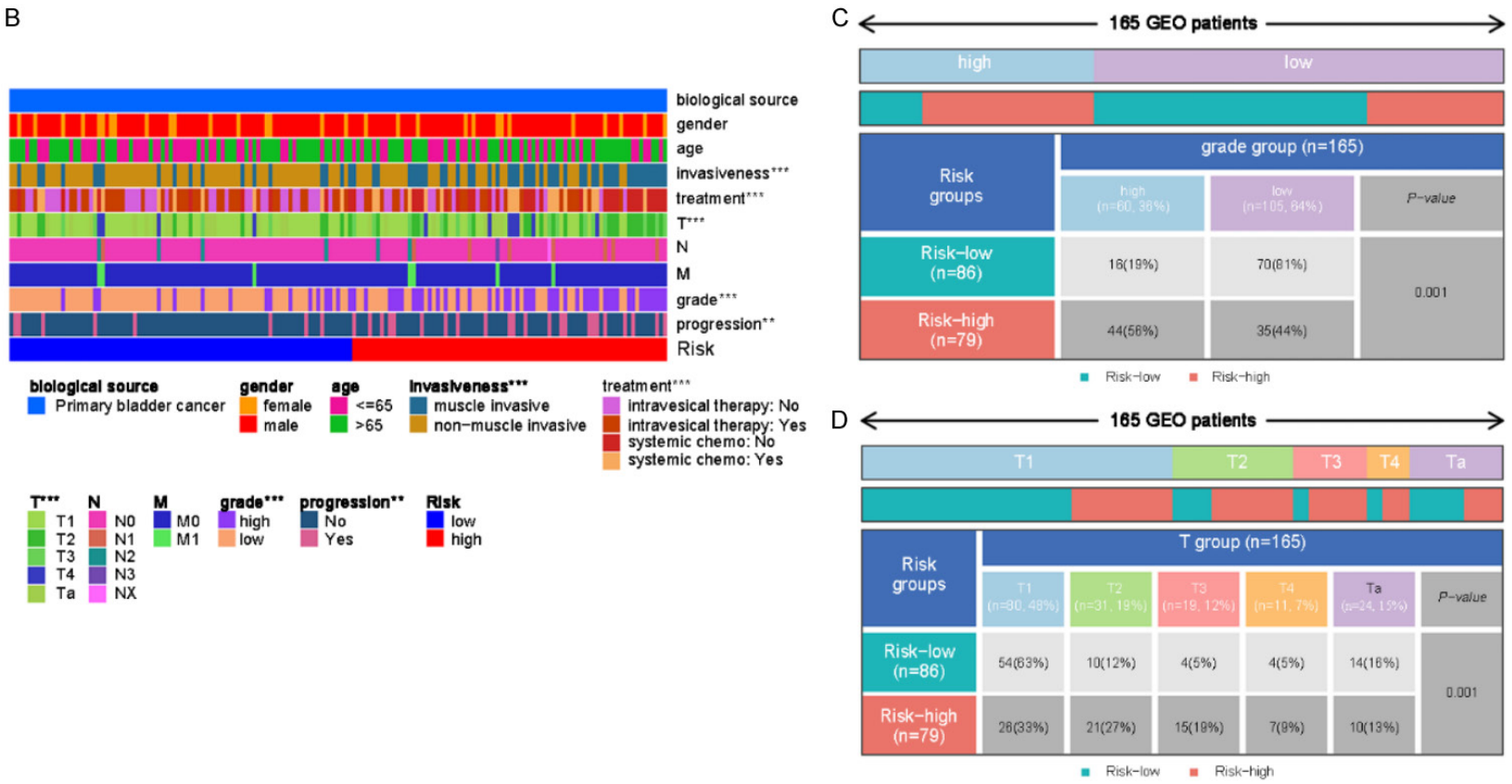

Figure 4. The HR group predicted the poor clinical features of BC patients. A. Heatmap of the 8 survival-related genes expression in HR and LR groups in GEO cohort. B. Heatmap of the correlation of clinical characteristics with the HR and LR groups in GEO cohort. C. Chi-square test for tumor grades and risk groups of BC samples in GEO cohort. D. Chi-square test for tumor T stages and risk groups of BC patients in GEO cohort.

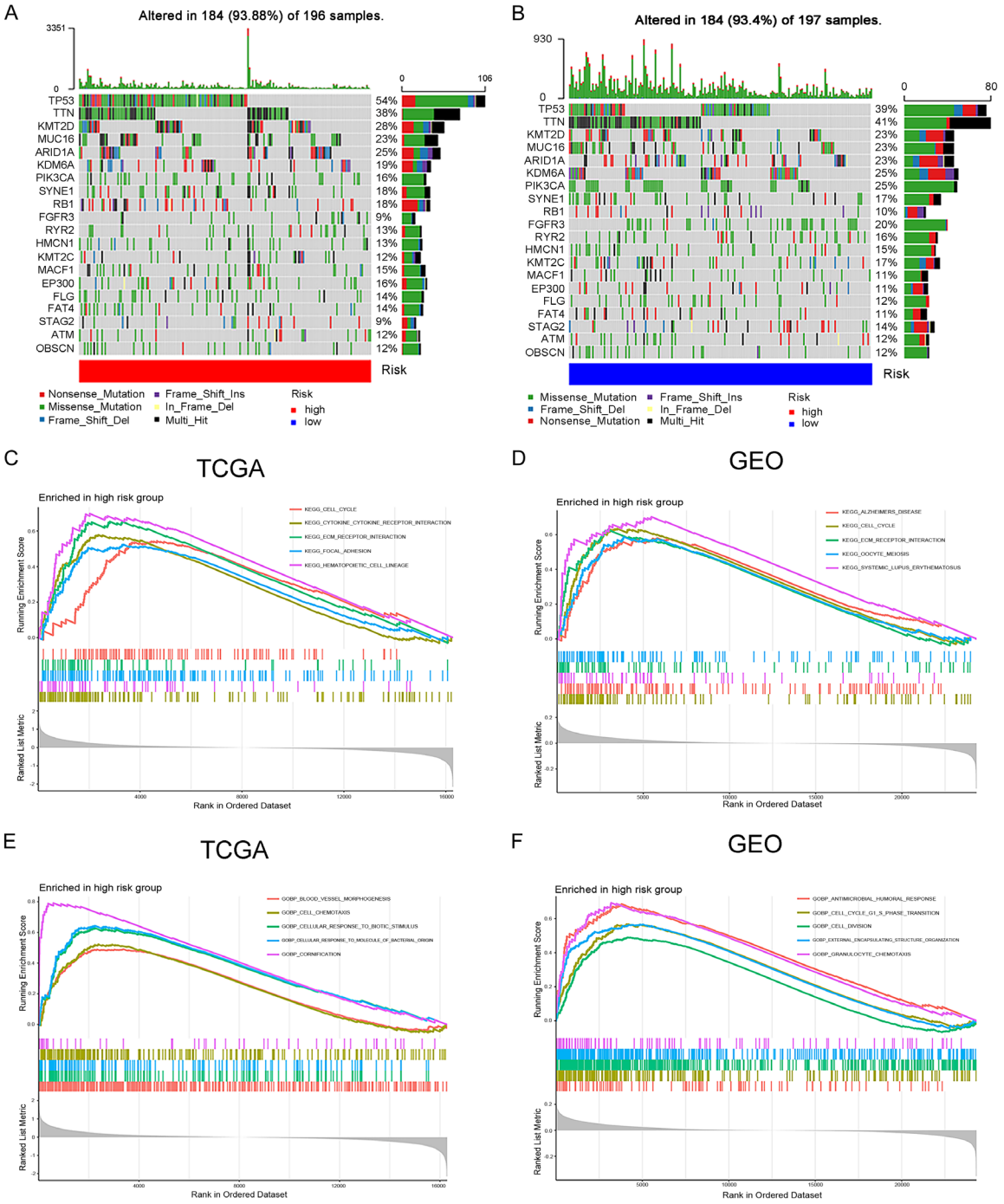

Figure 5. Gene mutation status and functional enrichment analysis for risk groups. A, B. Top 20 mutated genes in the HR and LR groups in TCGA cohort. C, D. KEGG enrichment analysis of the HR and LR groups in TCGA and GEO cohorts. E, F. GO enrichment analysis for the HR and LR groups in TCGA and GEO cohorts.

Gene mutation status and functional enrichment analysis

To assess the gene mutation status in these two risk groups, we used Maftools to analyze the gene mutation in all 393 BC samples from TCGA cohort, and the top 20 mutated genes in the HR and LR groups were listed in **Figure 5A** and **5B**, respectively. Overall, the HR and LR groups had similar total mutation frequencies

(93.88% vs 93.4%). However, TP53, the most frequently mutated gene in both risk groups, exhibited higher mutation rate in HR group than in LR group (54% vs 39%). Similarly, KMT2D mutation rate was also higher in HR group than in LR group (28% vs 23%). The high mutation rate of these genes might partially attribute to the poor prognosis of patients in the HR group.

Next, we applied GSEA enrichment analysis to further investigate the biological functions or pathways enriched in these two risk groups. KEGG enrichment analysis showed that pathways related to cell cycle, cytokine receptor interactions, and cell adhesion molecules were markedly enriched in the HR group of both TCGA and GEO cohorts (**Figure 5C**, **5D**; Supplementary Tables 2, 3). In addition, GO enrichment analysis showed that such cellular processes as cell response to biological stimulus, cell chemotaxis, regulation of humoral immune response, and negative regulation of immune system were highly enrichment in the HR group of both TCGA and GEO cohorts (**Figure 5E**, **5F**; Supplementary Tables 4, 5). Furthermore, 23 DEGs between the HR and LR groups of TCGA cohort, and 22 DEGs from the GEO cohort were identified. We then performed GO and KEGG enrichment analysis on these DEGs using DAVID software. We found that DEGs were mostly enriched in drug metabolic process, regulation of T cell migration, and chemokine activity in both TCGA and GEO cohorts (Supplementary Figure 2A, 2B), suggesting the difference in prognosis and immune function between the HR and LR groups of BC patients.

The HR group predicted a higher risk of immune escape

To further explore the difference in tumor immunity between the HR and LR groups, we investigated their correlation with clinical immune subtypes using the samples from TCGA cohort. The data showed that wound Healing (Immune C1) and IFN-gamma Dominant (Immune C2) were higher in the HR group than in the LR group (94% vs 78%), while Inflammatory (Immune C3) and Lymphocyte Depleted (Immune C4) were higher in the LR group than in the HR group (22% vs 7%) (P=0.001) (**Figure 6A**). These results further demonstrated the difference in immune response between HR and LR groups. Moreover, we investigated the composition of infiltrating immune cells and immune functions in these two risk groups from the TCGA cohort. We observed a lower level of NK cells and Th2 cells in the HR group, while a higher level of Treg cell, immune checkpoint, and T cell co-inhibitory signal in the HR group, suggesting the potential risk of immune escape in the HR group. Nevertheless, we also observed that some immune cell infiltration and immune response were higher in the HR group, suggesting the complexity of tumor microenvironment (**Figure 6B**, **6C**). Therefore, we evaluated the immune exclusion score of patients in the TCGA cohort and found that the HR group had a higher probability of immune exclusion (**Figure 6D**). Importantly, we examined the expression level of immune checkpoints such as PD-1, PD-L1, and CTLA4 in samples from both TCGA and GEO cohorts. Higher expression of PD-1, PD-L1, and CTLA4 was found in the HR group compared to the LR group (**Figure 6E-G**, Supplementary Figure 3A-C). Meanwhile, the risk score was significantly positively correlated with the expression levels of PD-1, PD-L1, and CTLA4 (**Figure 6E-G**, Supplementary Figure 3A-C). Taken together, our study suggested that patients in the HR group might suffer from immune escape and would be more likely to benefit from immunotherapy.

Discussion

Accumulating evidence has indicated that pyroptosis plays important roles in the development and progression of cancer. In our current study, we revealed the predictive value of pyroptosis in the prognosis of patients with BC. Importantly, we found that the expression of AIM2 and HMGB1 was significantly upregulated in BC in our cohorts. AIM2 is known as an innate immune sensor and can initiate pyroptosis to help prevent from infection. In support with this notion, the dysregulation of AIM2 is found to be closely associated with immune activity-related diseases and cancer [16]. HMGB1, as a nuclear protein, is involved in immune response and regulates apoptosis [17]. The dysregulation of HMGB1 is also reported to lead to inflammatory diseases and cancer [18].

In our study, we constructed a risk model with eight survival-related genes (KRT1, DSG3, PCOLCE2, ALDH1L2, CTSE, SULT1E1, GSDMB and BCL2L14). Among these genes, the expression of KRT1, DSG3, PCOLCE2, and ALDH1L2

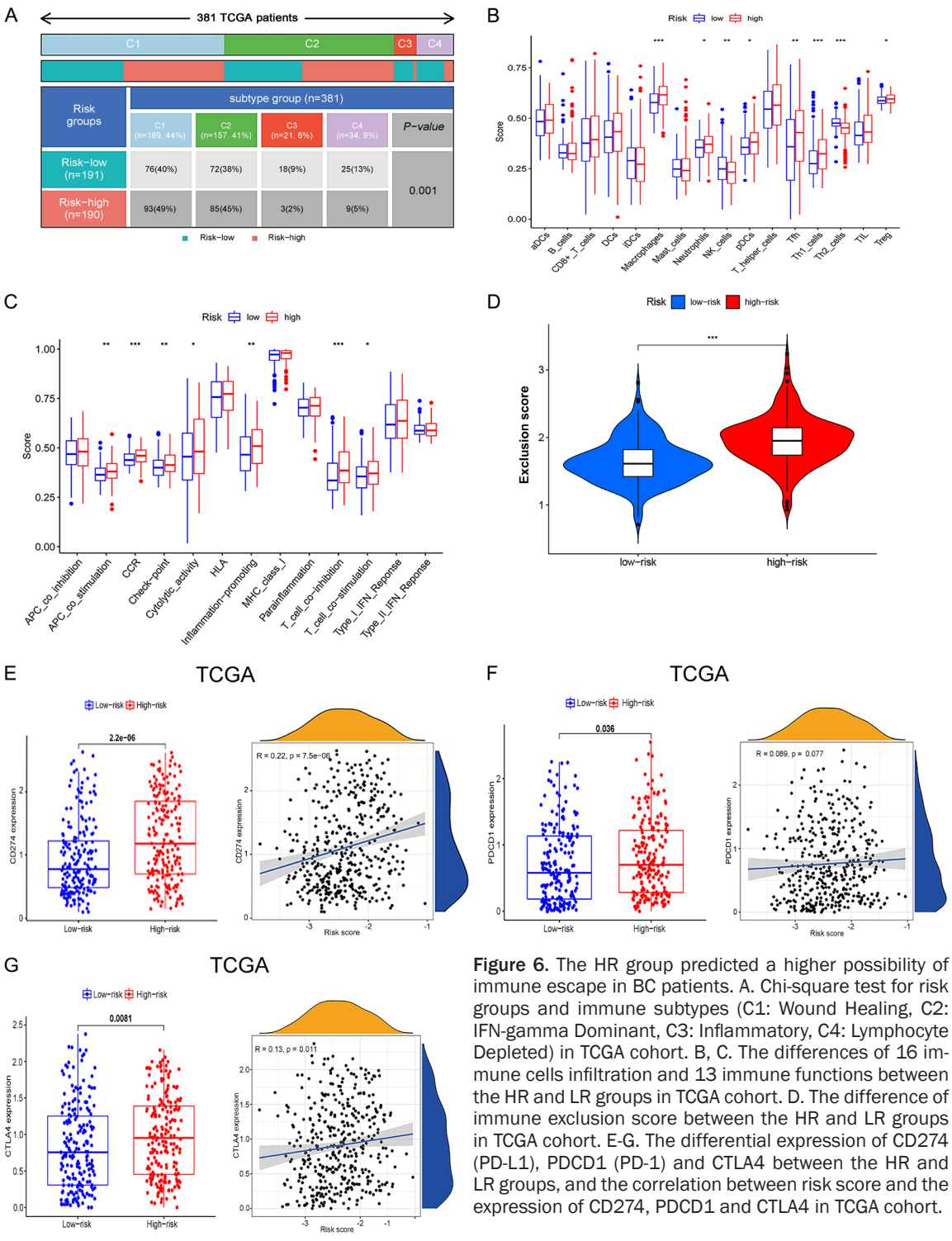

Figure 6. The HR group predicted a higher possibility of immune escape in BC patients. A. Chi-square test for risk groups and immune subtypes (C1: Wound Healing, C2: IFN-gamma Dominant, C3: Inflammatory, C4: Lymphocyte Depleted) in TCGA cohort. B, C. The differences of 16 immune cells infiltration and 13 immune functions between the HR and LR groups in TCGA cohort. D. The difference of immune exclusion score between the HR and LR groups in TCGA cohort. E-G. The differential expression of CD274 (PD-L1), PDCD1 (PD-1) and CTLA4 between the HR and LR groups, and the correlation between risk score and the expression of CD274, PDCD1 and CTLA4 in TCGA cohort.

was upregulated in the HR group. KRT1 has been reported to be associated with the aggressive subtype of BC [19], while DSG3 is a component of the desmosome involved in strong cell-cell adhesion and in the distinction of metastatic urothelial carcinoma [20]. PCOLCE2 is identified as a potential tumor marker, as the high expression of PCOLCE2 may attribute to tumorigenesis [21]. ALDH1L2 is a major member of folate-metabolizing enzymes, and the high expression of ALDH1L2 is reported to lead to poor OS and poor recurrence free survival of

colorectal tumor patients [22]. These findings were consistent with our data suggesting that high expression levels of these genes may associate with the occurrence and the poor prognosis of cancer patients.

In contrast, the other 4 genes (CTSE, SULT1E1, GSDMB and BCL2L14) used in our model were upregulated in the LR group. CTSE is reported to function in immune regulation, and high CTSE level may promote the chemoradiotherapy resistance and reduce the survival of rectal cancer patients [23]. However, in our study, BC patients in the LR group had higher expression of CTSE and better survival, which migh be due to the heterogeneity of the cancer and other unknown mechanisms. SULT1E1 is reported to inhibit the proliferation and invasion of breast cancer cells [24]. GSDMB is a key molecule participating in the regulation of pyroptosis and enhances the activity of cytotoxic lymphocyte, thereby stimulating anti-tumor immunity via regulating pyroptosis [25, 26]. BCL2L14 is a proapoptotic protein that activates and induces apoptosis, an important mechanism of antitumor activity [27]. These findings demonstrated the possible working mechanism of our risk model in predicting the prognosis of BC patients.

Regarding the gene mutations in our risk groups, we found that TP53 mutation rate was significantly higher in the HR group than in the LR group. Under normal circumstances, TP53 is a tumor suppressor gene and induces cell apoptosis when DNA damage occurs or cell cycle is arrested [28]. However, it has been reported that TP53 is one of the most frequently mutated genes in cancer and is associated with shorter OS of BC patients with TP53 mutation [29-31]. In our study, the HR group had higher TP53 mutation rate, which might be part of the reason for the poor prognosis in HR group. Furthermore, we found a lower level of NK cells and Th2 infiltration in the HR group, while a higher level of Treg cell, immune checkpoints, and T cell co-inhibitory signal in the HR group, which could be another mechanism for the poor prognosis of patients in the HR group. Surprisingly, compared with LR group, we observed that some infiltrating immune cells and immune responses were higher in the HR group. Since the roles of immune cell infiltration in cancer are complex, our observation of high immune cell infiltration in the HR group needs further investigation.

Immune checkpoint blockade therapy has been proven effective in many types of cancer including BC [32]. Cancer cells with high level of PD-1 and CTLA4 are correlated with inactivating tumor specific T cells and immune evasion, which attributes to poor prognosis [33]. Hence, treatment with anti-PD-1, anti-PD-L1, or anti-CTLA4 can enhance T cell function and anti-tumor immunity [34]. For example, it was reported that after receiving immunotherapy, the objective response rate was 26% in patients with high PD-L1 expression level, while it was only 4% in PD-L1 expression-low patients [35], indicating that PD-L1 expression level could predict immunotherapeutic response. In our study, we found higher expression levels of PD-1, PD-L1 and CTLA4 in the HR group in both TCGA and GEO cohorts, suggesting that the patients in HR group might benefit from immunotherapy; therefore, our model could potentially be used to predict the immunotherapeutic response in BC.

Conclusions

In conclusion, our results indicated that the pyroptosis-related gene signature could be used to predict the prognosis, TP53 mutation, and immune escape of patients with BC. These findings may also provide new potential targets for precision treatment of BC.

Acknowledgements

This study was supported by Horizontal project of Heilongjiang Renxin Medical Assistance Foundation and Natural Science Foundation of Heilongjiang Province (No. LH2019H030 to Ming-Hua Ren).

Disclosure of conflict of interest

None.

Abbreviations

BC, bladder cancer; DEGs, differentially expressed genes; HR group, high-risk group; LR group, low-risk group; TCGA, The Cancer Genome Atlas; GEO, Gene Expression Omnibus; LASSO, the least absolute shrinkage and selection operator; PPI, protein-protein interaction; GO, Gene ontology; KEGG, Kyoto Encyclopedia of Genes and Genomes; GSEA, Gene set enrichment analysis; ROC, Receiver operating character; AUCs, Area under curve; DSS, Disease specific survival; PFS, Progres-

sion-free survival; OS, Overall survival; DFS, Disease-free survival.

Address correspondence to: Ming-Hua Ren, Department of Urinary Surgery, First Affiliated Hospital of Harbin Medical University, Harbin 150007, Heilongjiang, China. Tel: +86-13946119939; E-mail: renminghua1972@163.com; Yu-Juan Shan, School of Public Health and Management, Wenzhou Medical University, Wenzhou 325000, Zhejiang, China. E-mail: yujuanshan@wmu.edu.cn

References

[1] Richters A, Aben KKH and Kiemeney LALM. The global burden of urinary bladder cancer: an update. World J Urol 2020; 38: 1895-1904.
[2] Siegel RL, Miller KD and Jemal A. Cancer statistics, 2019. CA Cancer J Clin 2019; 69: 7-34.
[3] DeGeorge KC, Holt HR and Hodges SC. Bladder cancer: diagnosis and treatment. Am Fam Physician 2017; 96: 507-514.
[4] Lenis AT, Lec PM, Chamie K and Mshs MD. Bladder cancer: a review. JAMA 2020; 324: 1980-1991.
[5] Kovacs SB and Miao EA. Gasdermins: effectors of pyroptosis. Trends Cell Biol 2017; 27: 673-684.
[6] Fang Y, Tian S, Pan Y, Li W, Wang Q, Tang Y, Yu T, Wu X, Shi Y, Ma P and Shu Y. Pyroptosis: a new frontier in cancer. Biomed Pharmacother 2020; 121: 109595.
[7] Xia X, Wang X, Cheng Z, Qin W, Lei L, Jiang J and Hu J. The role of pyroptosis in cancer: pro-cancer or pro-"host"? Cell Death Dis 2019; 10: 650.
[8] Chen X, Chen H, Yao H, Zhao K, Zhang Y, He D, Zhu Y, Cheng Y, Liu R, Xu R and Cao K. Turning up the heat on non-immunoreactive tumors: pyroptosis influences the tumor immune microenvironment in bladder cancer. Oncogene 2021; 40: 6381-6393.
[9] Fu J and Wang Y. Identification of a novel pyroptosis-related gene signature for predicting prognosis in bladder cancer. Cancer Invest 2022; 40: 134-150.
[10] Zhou TC, Sankin AI, Porcelli SA, Perlin DS, Schoenberg MP and Zang X. A review of the PD-1/PD-L1 checkpoint in bladder cancer: from mediator of immune escape to target for treatment. Urol Oncol 2017; 35: 14-20.
[11] Song D, Powles T, Shi L, Zhang L, Ingersoll MA and Lu YJ. Bladder cancer, a unique model to understand cancer immunity and develop immunotherapy approaches. J Pathol 2019; 249: 151-165.
[12] Powles T, Eder JP, Fine GD, Braiteh FS, Loriot Y, Cruz C, Bellmunt J, Burris HA, Petrylak DP, Teng SI, Shen X, Boyd Z, Hegde PS, Chen DS and Vogelzang NJ. MPDL3280A (anti-PD-L1) treatment leads to clinical activity in metastatic bladder cancer. Nature 2014; 515: 558-562.
[13] Brosh R and Rotter V. When mutants gain new powers: news from the mutant p53 field. Nat Rev Cancer 2009; 9: 701-713.
[14] Wu X, Lv D, Cai C, Zhao Z, Wang M, Chen W and Liu Y. A TP53-associated immune prognostic signature for the prediction of overall survival and therapeutic responses in muscle-invasive bladder cancer. Front Immunol 2020; 11: 590618.
[15] Ardeshir-Larijani F, Bhateja P, Lipka MB, Sharma N, Fu P and Dowlati A. KMT2D mutation is associated with poor prognosis in non-small-cell lung cancer. Clin Lung Cancer 2018; 19: e489-e501.
[16] Lugrin J and Martinon F. The AIM2 inflammasome: sensor of pathogens and cellular perturbations. Immunol Rev 2018; 281: 99-114.
[17] Huebener P, Gwak GY, Pradere JP, Quinzii CM, Friedman R, Lin CS, Trent CM, Mederacke I, Zhao E, Dapito DH, Lin Y, Goldberg IJ, Czaja MJ and Schwabe RF. High-mobility group box 1 is dispensable for autophagy, mitochondrial quality control, and organ function in vivo. Cell Metab 2014; 19: 539-547.
[18] Wang S and Zhang Y. HMGB1 in inflammation and cancer. J Hematol Oncol 2020; 13: 116.
[19] Mehus AA, Bergum N, Knutson P, Shrestha S, Zhou XD, Garrett SH, Sens DA, Sens MA and Somji S. Activation of PPARγ and inhibition of cell proliferation reduces key proteins associated with the basal subtype of bladder cancer in As3+-transformed UROtsa cells. PLoS One 2020; 15: e0237976.
[20] Gruver AM, Amin MB, Luthringer DJ, Westfall D, Arora K, Farver CF, Osunkoya AO, McKenney JK and Hansel DE. Selective immunohistochemical markers to distinguish between metastatic high-grade urothelial carcinoma and primary poorly differentiated invasive squamous cell carcinoma of the lung. Arch Pathol Lab Med 2012; 136: 1339-1346.
[21] Yao H, Li C and Tan X. An age stratified analysis of the biomarkers in patients with colorectal cancer. Sci Rep 2021; 11: 22464.
[22] Krupenko SA and Krupenko NI. ALDH1L1 and ALDH1L2 folate regulatory enzymes in cancer. Adv Exp Med Biol 2018; 1032: 127-143.
[23] Chou CL, Chen TJ, Tian YF, Chan TC, Yeh CF, Li WS, Tsai HH, Li CF and Lai HY. CTSE overexpression is an adverse prognostic factor for survival among rectal cancer patients receiving CCRT. Life (Basel) 2021; 11: 646.
[24] Xu Y, Lin X, Xu J, Jing H, Qin Y and Li Y. SULT1E1 inhibits cell proliferation and invasion by acti-

vating PPARγ in breast cancer. J Cancer 2018; 9: 1078-1087.
[25] Zhou Z, He H, Wang K, Shi X, Wang Y, Su Y, Wang Y, Li D, Liu W, Zhang Y, Shen L, Han W, Shen L, Ding J and Shao F. Granzyme A from cytotoxic lymphocytes cleaves GSDMB to trigger pyroptosis in target cells. Science 2020; 368: eaaz7548.
[26] Li L, Li Y and Bai Y. Role of GSDMB in pyroptosis and cancer. Cancer Manag Res 2020; 12: 3033-3043.
[27] Guo B, Godzik A and Reed JC. Bcl-G, a novel pro-apoptotic member of the Bcl-2 family. J Biol Chem 2001; 276: 2780-2785.
[28] Lai PB, Chi TY and Chen GG. Different levels of p53 induced either apoptosis or cell cycle arrest in a doxycycline-regulated hepatocellular carcinoma cell line in vitro. Apoptosis 2007; 12: 387-393.
[29] Ingaramo MC, Sánchez JA and Dekanty A. Regulation and function of p53: a perspective from drosophila studies. Mech Dev 2018; 154: 82-90.
[30] Nassar AH, Umeton R, Kim J, Lundgren K, Harshman L, van Allen EM, Preston M, Dong F, Bellmunt J, Mouw KW, Choueiri TK, Sonpavde G and Kwiatkowski DJ. Mutational analysis of 472 urothelial carcinoma across grades and anatomic sites. Clin Cancer Res 2019; 25: 2458-2470.
[31] Sjödahl G, Eriksson P, Patschan O, Marzouka NA, Jakobsson L, Bernardo C, Lövgren K, Chebil G, Zwarthoff E, Liedberg F and Höglund M. Molecular changes during progression from nonmuscle invasive to advanced urothelial carcinoma. Int J Cancer 2020; 146: 2636-2647.
[32] Rosenberg JE, Hoffman-Censits J, Powles T, van der Heijden MS, Balar AV, Necchi A, Dawson N, O'Donnell PH, Balmanoukian A, Loriot Y, Srinivas S, Retz MM, Grivas P, Joseph RW, Galsky MD, Fleming MT, Petrylak DP, Perez-Gracia JL, Burris HA, Castellano D, Canil C, Bellmunt J, Bajorin D, Nickles D, Bourgon R, Frampton GM, Cui N, Mariathasan S, Abidoye O, Fine GD and Dreicer R. Atezolizumab in patients with locally advanced and metastatic urothelial carcinoma who have progressed following treatment with platinum-based chemotherapy: a single-arm, multicentre, phase 2 trial. Lancet 2016; 387: 1909-1920.
[33] Krummel MF and Allison JP. CD28 and CTLA-4 have opposing effects on the response of T cells to stimulation. J Exp Med 1995; 182: 459-465.
[34] Pardoll DM. The blockade of immune checkpoints in cancer immunotherapy. Nat Rev Cancer 2012; 12: 252-264.
[35] Powles T, O'Donnell PH, Massard C, Arkenau HT, Friedlander TW, Hoimes CJ, Lee JL, Ong M, Sridhar SS, Vogelzang NJ, Fishman MN, Zhang J, Srinivas S, Parikh J, Antal J, Jin X, Gupta AK, Ben Y and Hahn NM. Efficacy and safety of durvalumab in locally advanced or metastatic urothelial carcinoma: updated results from a phase 1/2 open-label study. JAMA Oncol 2017; 3: e172411.

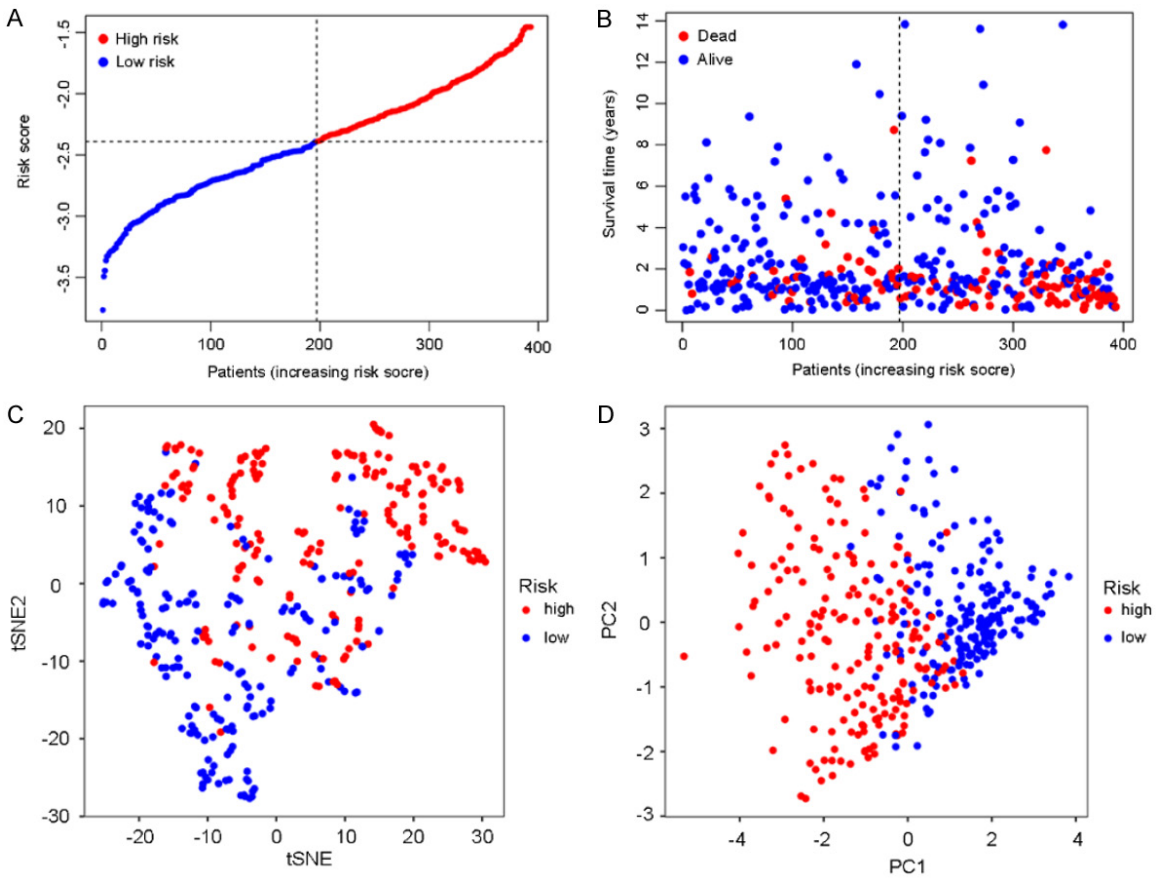

Supplementary Figure 1. A. BC cases were separated into HR group and LR group by median risk score in TCGA cohort. B. Living status of BC cases in TCGA cohort. C, D. tSNE and PCA plot based on risk scores.

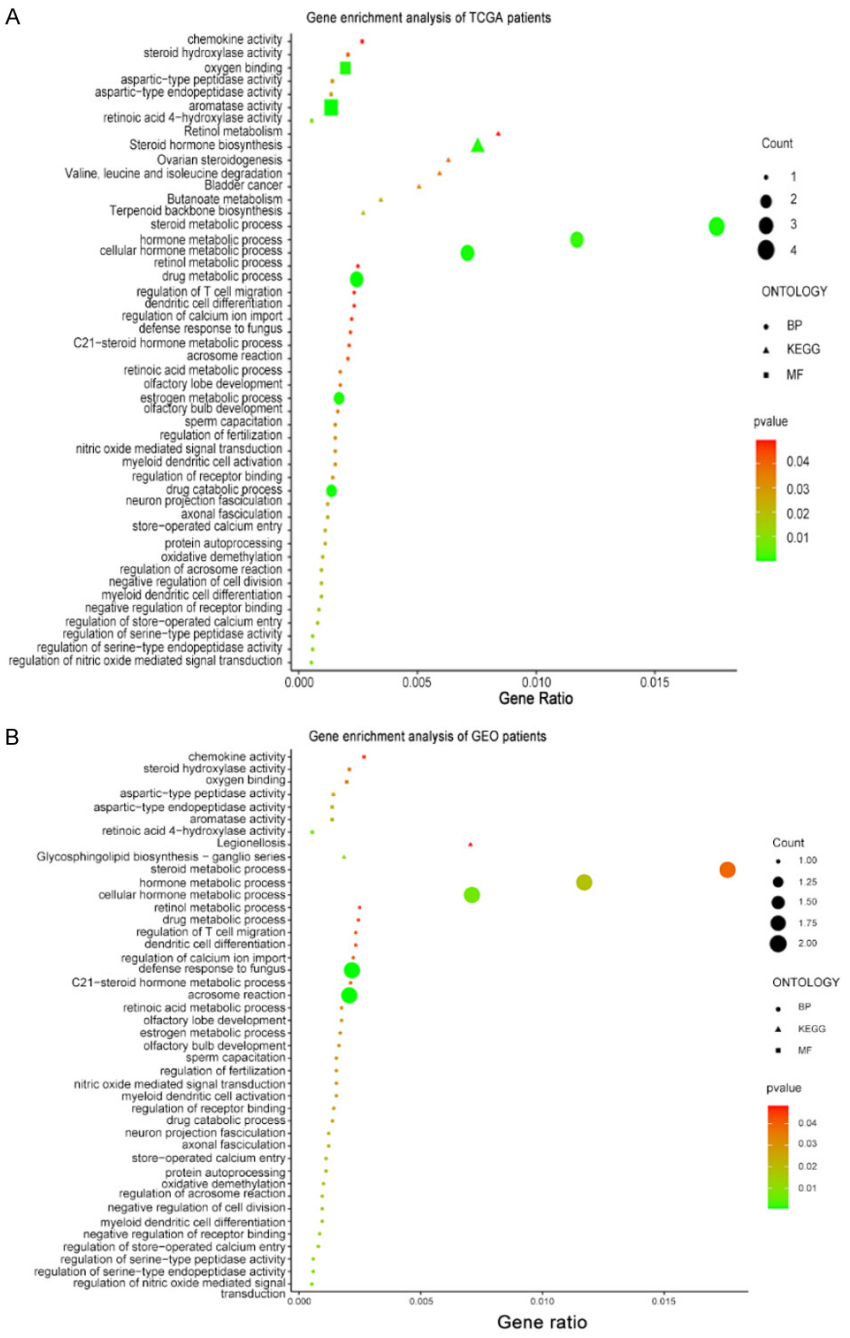

Supplementary Figure 2. A. GO and KEGG enrichment analysis were performed based on DIVID for the DEGs of HR and LR groups in TCGA cohort. B. GO and KEGG enrichment analysis were performed based on DIVID for the DEGs of HR and LR groups in GEO cohort.

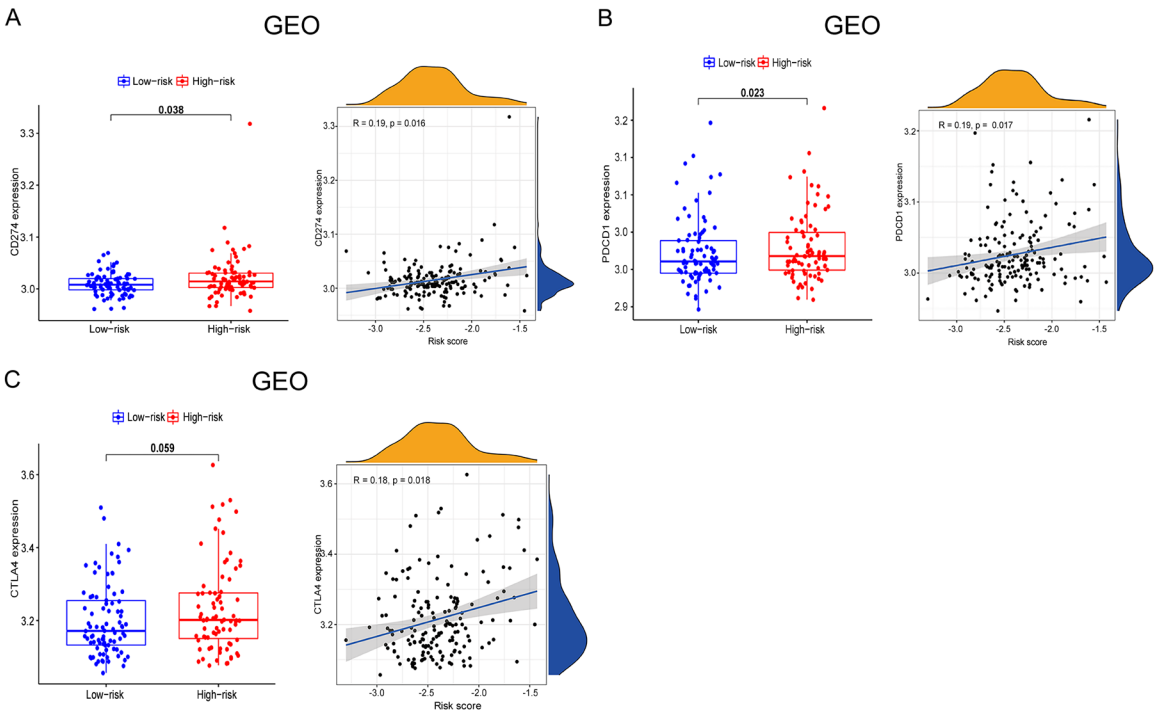

Supplementary Figure 3. A-C. The expression differences of CD274 (PD-L1), PDCD1 (PD-1) and CTLA4 in HR and LR groups, and correlations between risk score and CD274, PDCD1 and CTLA4 expression level in GEO cohort.